NASA TECHNICAL
MEMORANDUM

NASA TM X-62,026

NASA TM X-62,026

LUNAR FOSSIL MAGNETISM AND PERTURBATIONS OF THE SOLAR WIND

C. P. Sonett and J. D. Mihalov

Ames Research Center
Moffett Field, Calif. 94035

June 1971

LUNAR FOSSIL MAGNETISM AND PERTURBATIONS OF THE SOLAR WIND

C. P. SONETT

J. D. MIHALOV

Ames Research Center, NASA

Moffett Field, California 94035

ABSTRACT

Perturbations of the solar wind downstream of the moon and lying outside of the rarefaction wave which defines the diamagnetic cavity are used to define possible source regions comprised of intrinsically magnetized areas of the moon. A map of the moon is constructed showing that a model where the sources are exposed to the grazing solar wind during the lunation yields a selenographically invariant set of regions strongly favoring the lunar highlands over the maria. An alternative model with the source due to electromagnetic induction is explored. The ages of the field sources should be consistent with those based upon the basalt ages, and possibly far older if the sources are connected with the formation of the highland rocks themselves. The perturbations are tentatively identified as weak shock waves, and a Mach angle in accord with nominal values for the solar wind is found.

INTRODUCTION

The primary perturbations induced in the interplanetary magnetic field by the presence of the moon are those associated with the formation of the diamagnetic cavity on the hemisphere shielded from direct impact of the solar wind. In addition to the rarefaction wave at the edges of the cavity and the diamagnetic increase sometimes seen inside of the cavity [Colburn et al., 1967; Ness et al., 1967], there appears to be a noise field surrounding the moon which is observed on field lines which jointly intersect the satellite where the observation is made and the moon [Ness and Schatten, 1969] and lastly an apparently sporadic increase in the magnetic field adjoining the rarefaction wave and invariably lying on the solar wind side of the wave [Ness et al., 1968; Colburn et al., 1971].

Attempts to explain the latter phenomenon have taken two basic forms. Ness et al. [1968] and Whang [1968] have proposed that they are a natural manifestation of the cavity formation and are associated with and due to plasma characteristics, and that the influence of the moon enters solely through its geometrical target cross section which is responsible for the cavity formation in the first place. This has been criticized by Schwartz et al. [1969] who proposed that the perturbations are a result of an interaction of the solar wind with the limb of the moon. The latter supposes that a weak unipolar interaction takes place which can vary depending upon the total circuit impedance on a path which both threads the moon locally and closes at both ends in direct contact with the solar wind. Such a mechanism cannot be ruled out at the present time, but recent investigation of the whole body statistics with special reference to the question of unipolar induction indicated that this mechanism is not favored [Colburn et al., 1971]. On the other hand, data from the Lunar Surface Magnetometer (LSM) show that a contribution to the whole body induction from the unipolar or TM (transverse magnetic) mode cannot be ruled out [Sonett et al, 1971a; 1971b]. Whang [1969] has also suggested that the perturbations discussed here are due to the permeability change at the solar wind-lunar surface boundary.

Recently we reported a different approach in attempting to identify the sources for the perturbation, still assuming that they are a lunar property and come into play as the perturbation source is exposed on the lunar limb to the grazing interaction of the solar wind [Mihalov et al., 1971]. The hypothesis employed is that the sources are located in sites which are permanently magnetized on the surface of the moon or at depths sufficiently small so that fields exist above the surface.

The model is suggested by the pervasive appearance in lunar rocks of fossil magnetism (cf. Proceedings of the Lunar Science Conferences), and the steady fields measured both by the LSM at the Apollo 12 landing site [Dyal et al., 1970] and also by the lunar portable magnetometer (LPM) at two sites near the Apollo 14 landing area [Dyal et al., 1971]. Thus convincing evidence is present for the widespread appearance of fields on the lunar surface. The microscale magnetic features suggested by the Apollo experiments are augmented in this paper by a model where mesoscale sources also exist, which the Explorer data is particularly suitable for detecting; in addition, Barnes et al. [1971] argue that the microscale features do not produce observable limb shocks.

The Apollo evidence indicates that the field sources are likely very old, corresponding at least to the ages of the marial basalts. The association of the perturbations studied here with highland features on the moon suggest that some of the magnetizing episodes may well be older than the 3.2 to 3.7 billion year ages inferred from the Rb/Sr dating of the basalts [Papanastassiou and Wasserburg, 1971].

There is presently no positive indication of a global magnetic field on the moon. Explorer bounds imply an upper limit of less than 10^{20} gauss-cm^3 equivalent to an upper limit surface field of 2 gamma for a centered dipole [Sonett et al., 1967; Behannon, 1968; see also Mihalov and Sonett, 1971]. Thus the manifestations studied here suggest identification with local areas of magnetization. The key result shown here is the selenographic invariance of the perturbations when used in a model where the sources are taken to be fixed on the moon. We also show that the perturbations are consistent with a weak shock wave by indicating a plausible Mach angle for them.

DATA

All data reported in this paper have been taken with the Ames magnetometer employing synchronous spin demodulators in the spacecraft operating upon the two signals derived from the spin plane sensors. The demodulators remove the spin modulation and can be shown to lead to signals formally identical to those taken from an attitude stabilized spacecraft where spin modulation lines are absent from the Fourier spectra of the component signals [Sonett, 1966]. Presampling filters are used to limit the alias to 0.1% based upon a white noise background; they are also shaped to preserve the pulse response of the signal, i.e., approximating linear phase shift with frequency. Sampling is done on all three axes over a time period short compared to the presample bandwidth and the Nyquist frequency is determined by the longest of the nearly equal sampling intervals (cf. Sonett [1968]).

The data reported covers the time interval from launch (July 1967) to April 16, 1970 extending our earlier reporting interval by 11 months. Data from each passage of the spacecraft in or out of the diamagnetic cavity are examined during this interval. Those transits for which a single positive excursion of the field occurs just adjacent and exterior to the rarefaction wave are tabulated, provided that the peak signal amplitude is equal to or greater than 0.7 gamma. Subsidiary requirements are that the principal perturbation be clean and free of obvious secondary variations. In the previous report [Mihalov et al., 1971] 7.4% of all transits, excluding data gaps, were observed to possess perturbations satisfying similar criteria. In the extension reported here this value is unchanged; 7.4% of all transits, excluding data gaps, show perturbations satisfying the stated criteria.

Four specific examples of perturbations having a magnitude greater than or equal to 0.7 gamma are shown in Figure 1. This figure shows the traces of the field magnitude, and in each case the optical shadow which defines the optical terminator, and convincingly shows the diamagnetic cavity and the associated rarefactions in the field discussed earlier [Colburn et al., 1967; Ness et al., 1967; Colburn et al., 1971]. In all four cases the perturbation seen just prior to spacecraft entrance into the shadow region is clearest and only those cases are counted in accordance with the criteria given above. A selenographic invariance of the cases selected for this illustration is demonstrated by noting that 21 months separates the earliest and latest observations, and that the projected locations on the lunar surface indicated for each entry perturbation are in the same general region.

SELENOGRAPHIC MAPPING ONTO THE LUNAR SURFACE

The basic geometry for projection of the perturbation upon the lunar surface follows that reported earlier [Mihalov et al., 1971]. The scheme is given in Figure 2 showing the idealized aberrated solar wind direction, the location of Explorer 35 downwind of the moon, the perpendicular erected from the solar wind vector passing through Explorer 35 to the lunar surface, and the locus of the hypothetical shock surface. The shading indicates the optical terminator, while the solar wind terminator is defined by the great circle upon the moon which divides it into hemispheres exposed to and shadowed from the solar wind.

Figure 3 gives the inferred individual source locations projected upon the moon according to the goemetry shown in the previous figure. Those cases where plasma data are available to us at this time are indicated by triangles. Error limits in the selenographic location upon the moon and due to solar wind flow direction uncertainties about the typical values assumed for the projections where plasma data is not available are estimated to be about ±5°. An additional uncertainty arises from the cylindrical symmetry about the flow direction expected for a limb shock wave on the moon; we have not developed information regarding the latitude on the shock surface appropriate to each observation of an exterior maximum. This uncertainty is reflected primarily in the selenographic latitude for the inferred sources. On Figure 3, slash marks indicate individual source locations due to perturbations observed more than 2.1 R_m (lunar radii) downstream, for which this uncertainty is greatest. (For these cases, the latitude limits associated with the uncertainties in the locations of the points may exceed $\pm 90^\circ \times 2.1\ R_m \times \tan 7^\circ \sim \pm 23^\circ$.)

A representation that is more commensurate with errors associated with the individual observations is given by clustering the surface locations and to weight the occurrences by the total number of scans over the surface. This is shown in Figure 4 which is similar to the map given in Mihalov et al. [1971] but includes the additional information developed in this paper by using the approximately 50% increase in time. The added data are all within 30° of the equator with more samples at eastern longitudes than western. The results are similar and differ only in detail. Concentrations are seen near 20° S latitude and 135° E to 170° W longitude on the lunar far side. The primary difference from the earlier map is the addition of sources at 5°-10° N latitude and 160°-180° W longitude. Scans from cases where Explorer was more than 4.0 R_m downstream of the moon were not included in the previous map but are included here. For this paper an average of 2 samples per 10^5 km^2 area on the lunar surface between 45° and 60° N latitude has been assigned; the corresponding value is 4 for the region between 45° and 60° S latitude. These values are 8 and 2 for the 60° of latitude centered on the equator, and the remaining surface area within 45° of the equator, respectively. The reference area of 10^5 km^2 represents about 80% of the area of 15° of longitude in the 45° to 60° latitude range, and about one-half the area of 15° of longitude in the 0° to 15° latitude range.

In the scanning process all regions of the moon are covered since the orbit of Explorer 35 has both major and minor axes tipped out of the plane of the ecliptic; this together with the lunar monthly and annual motion of the Earth-moon system about the Sun and precession of periselene produces the required coverage. Nevertheless no sources are located in polar regions, i.e., more than 45° in latitude away from the equator, though we cannot exclude the possibility that some geometrical bias exists which discriminates against seeing polar sources.

The application of the stringent criteria deleting all cases having perturbations less than 0.7 gamma excluded cases used in some earlier reports [Schwartz et al., 1969; Colburn et al., 1971] where smaller perturbations were included. Although these may have been real, the infrequent occurrence of the larger events is the basic reason why the ordering in the present data could not be made until this time. The cases used in this paper confirm the selenographic invariance on the lunar surface lending strong support to the view that a lunar limb perturbation depending upon a set of fixed features on the moon is responsible for the events.

Mihalov et al. [1971] presented calculated probabilities that there is no concentration of inferred source locations at seven regions on the lunar surface. These probabilities have been recalculated using the added data presented in this paper, and the results are compared in Table 1. The probability increased for one region (the most concentrated region, and also the one associated with the observations presented in Figure 1 of this paper). The probabilities remain approximately constant for region 3, and decrease for the remaining five regions. With the added data, region 6 no longer demonstrates a clear concentration of source locations. Region 6 is a small highland area chosen where there were source locations from the earlier collection of data. The more recent data adds new source locations in the adjacent highland regions that reduces the concentration probability as shown for the old region. With the added source locations, a new region of concentration combining regions 6 and 7 at least should be used in such calculations.

PROPERTIES OF THE PERTURBATIONS

In Figure 5 we show a set of downstream locations of Explorer 35 where the perturbations are noted. These are comprised of the observations from July 1967 to May 1969 discussed previously [Mihalov et al., 1971]. The measured plasma flow direction has been used in making this graph for the 18 cases indicated by squares where data is available while the idealized 4° aberration of the solar wind is assumed for the remaining cases. Stated another way the plasma flow directions, either measured or inferred, are used as the abscissae for plotting; thus the deviations from a constant value of the ordinate suggest the propagation of a wave. The observations are presented in a common plane with the ordinate taking the value of the perpendicular distance of the point where the observation was made from the flow direction ray passing through the center of the moon. Observations before entering the lunar shadow are given at the top of Figure 5 while those upon exit are shown at the bottom.

Table 1. Calculated probabilities for seven regions on the lunar surface that there is no concentration of source locations.

Seleocentric latitude	Selecocentric longitude	Calculated probability: July 1967 - May 1969 (excludes samples beyond $4R_m$)	Calculated probability: July 1967 - April 1970
1. 5 - 20 S	135 E - 165 W	4×10^{-14}	4×10^{-15}
2. 6 N	88 W	5×10^{-7}	3×10^{-5}
3. 0 - 20 N	60 - 115 E	3×10^{-3}	2×10^{-3}
4. 5 S	138 W	6×10^{-3}	2×10^{-3}
5. 2 N	35 W	1×10^{-6}	1×10^{-5}
6. 5 N	0	5×10^{-4}	0.2
7. 0	25 E	4×10^{-5}	2×10^{-4}

Mach lines are indicated by both the sets of observations taken using the measured plasma flow vector and the inferred value of aberration. Least-squares fits of straight lines for both the inbound and outbound observation locations indicated by the dashed lines in Figure 5 give angles to the flow direction of $7°49' \pm 1°40'$ and $6°33' \pm 1°54'$, respectively. Observations with plasma data are weighted twice as heavily as those without because of the smaller uncertainty in the projection for these cases. Using all the data as one set yields an angle of $7°26' \pm 1°19'$. These angles are smaller than the one case of 19° reported earlier by Siscoe et al. [1969].

The minimum distance to the moon's surface for the inbound and outbound Mach lines described above (dashed lines on Figure 5), are $0.231 \pm 0.053\ R_m$ and $0.197 \pm 0.058\ R_m$, respectively. Using the cases with plasma data alone the Mach angle is 13° and the minimum distance from the lunar surface is reduced to 0.03 R_m. We have also taken these 18 cases together with the complete plasma parameters and the magnetic field direction and calculated the fast and slow [Jeffrey and Taniuti, 1964] and Alfvén and sonic speeds. The number of samples is limited, and consideration of these propagation angles does not reduce the scatter of the 18 points from a linear least-squares fit, except possibly for the sonic speed. The complete set of exterior perturbation observations from Figure 5 do exhibit anisotropic propagation of the disturbance, about the same as the results reported by Whang and Ness [1970] for the rarefaction region. The average fast, slow, Alfvén and sonic Mach angles are 10.7°, 2.6°, 9.3° and 5.8°, respectively. We think it likely that the events witnessed are due to a weak shock wave. Since, as shown later, there is evidence that the thickness of the perturbation in the solar wind is of order 200 km, it is entirely reasonable to conclude that the resolution of the geometry together with the unavoidable scatter in the solar wind plasma parameters when unavailable cannot more accurately define the distance of the closest approach of the perturbation to the surface of the moon. Residual scatter may indicate latitudes of shock traversals.

The exact form of the perturbation near the surface is inaccessible to this experiment. Differences are likely present between attached and free-standing MHD shocks due to boundary conditions at the surface; there are also fundamental uncertainties associated with microscopic features of solar wind deflection by surface magnetism discussed by Barnes et al. [1971].

Barnes et al. [1971] have discussed the relation to the scaled distance from the source of the amplitudes of weak perturbations due to shocks. The relative amplitude $\Delta|\vec{B}|/|\vec{B}|$ for the 38 pronounced exterior maxima observed during March 19 to September 29, 1968 are plotted against distance downstream in Figure 6. Most of the relative amplitudes are less than 50%, and while the largest values are within 1.2 R_m downstream, there is no other evidence than this for a decrease or other systematic change of the relative amplitudes with distance. In Figure 7 the duration of the time record of these exterior peaks is plotted with respect to distance downstream. Increased durations are suggested for increasing distance downstream. This tendency is more pronounced when a set of observations associated with just one location on the lunar surface is considered. However, this suggested effect is the same as that expected from the decreased speed of the satellite at greater selenocentric distances, so no change in size is implied for the enhanced field region. The typical full width at half maximum of the exterior field peak in the solar wind is ~200 km. However, this observation does not imply a width for the source region on the lunar surface. At the lunar surface, a relative amplitude of

~ 1 is implied for a scale size of 5° of latitude associated with the observations projected onto a region on the lunar surface from 128° to 144° East longitude and 13° to 25° South latitude [Barnes et al., 1971], and for smaller scale sizes. The profiles of these large exterior peaks are generally much more gradual at greater distances. The increase in field magnitude on the side away from the cavity is typically steeper than the decrease toward the cavity signature, but is not so abrupt so as to necessarily suggest a shock.

Figure 8 gives the dependence with distance downstream from the moon of the fraction of observations with large exterior maxima, for the 561 cases from March 18 to October 30, 1968. The distribution of selenographic latitudes scanned for various distances downstream for this time period is also given. A steep decrease of the fraction of all scans that exhibit exterior peaks occurs at about 3.5 R_m downstream, as indicated on Figure 8. At smaller downstream distances than that of the decrease, there are already numerous scans of the lunar surface at latitudes more than 30° from the equator where no source locations for exterior peaks have been found. This suggests that the lack of source locations nearer the poles is a real, separate effect from the decline in incidence of exterior peaks farther downstream than 3.5 R_m, although this latter effect should produce a discrimination against the polar regions. In the earlier publication [Mihalov et al., 1971], scans at distances beyond 4 R_m were not used. We cannot eliminate the possibility that field lines blown back from the lunar surface contribute to the exterior peaks observed closest to the moon, and termination of such field lines could be involved with the apparent attenuation of exterior peak occurrence with downstream distance indicated by Figure 8.

Ness and Schatten [1969] observed noisy magnetic fields with amplitudes of several gamma peak-to-peak near the moon when Explorer 35 was located on magnetic field lines that intersect the plasma penumbra along the rectilinear extension. The possibility has been considered that extreme cases of these oscillations might affect the observations of exterior maxima that are discussed here. For 64% of the July 1967 to May 1969 observations of exterior maxima discussed previously [Mihalov et al., 1971] Explorer 35 is located on magnetic field lines that do not connect to the plasma penumbra.

We have searched for direct evidence of localized lunar magnetism using periselene data from Explorer 35. At selected times in the geomagnetic tail, the fluctuations in the ambient magnetic fields observed by this spacecraft are smaller than the experimental digitization window width, for periods as long as tens of minutes. Periselene occurs in the geomagnetic tail over the most concentrated source locations on the moon's far side only during telemetry occultation, so no data is available to use in such tests. Turning to the moon's front side, Figure 9 gives an example of unusually quiet geomagnetic tail data when periselene was at 6° N and 102° E at the Eastern limb of the moon, above a concentration of source locations. The upper limit moment for an arbitrarily oriented dipole on the lunar surface, beneath the lowest portion of the satellite orbit, is 2×10^{18} G-cm^3 from this one pass. The limit is set by the ±0.2 gamma experimental digitization window width.

A somewhat more useful measure is the fraction of the surface magnetic flux density along the axis far ($d >> t$) from a disk (radius r, thickness t) uniformly magnetized parallel to its axis. This fraction is given approximately by

$\left[1 + (d^2/r^2)\right]^{-1}$ for $r^2 >> t^2$. The example of Figure 9 implies an ~80 gamma limit for surface field strengths for a 350 km diameter disk source centered near 6° N and 102° E. A ~10 km minimum scale size [Barnes et al., 1971] would permit an upper limit of ~0.1 G to the surface field strength; the origin for field strengths of this magnitude would not be clear and they are not expected. There are other examples of quiet tail field data at periselene above different equatorial near-side locations. These examples do not decrease the upper limit previously stated from Explorer 35 data, for lunar surface fields due to a centered dipole.

DISCUSSION

Observed features of exterior peaks

The basis for the inference regarding the source of the perturbations in the magnetic field is seated in the argument that they invariably lie just outside of the rarefaction wave which defines the edge of the diamagnetic cavity. The rarefaction possesses a speed defined by the magnetosonic velocity calculated from the values of solar wind plasma parameters which exist at the time of the observation [Whang and Ness, 1970]. If the perturbations discussed in this paper are due to a wave, then clearly the wave must be supersonic since it lies outside of the rarefaction. If not a wave, then it is a sporadic event convected in the solar wind. Its occasional appearance is explained by the latter supposition, but its persistent position just outside the rarefaction appears to be governed by more than chance. Also the data sample is taken with a bias towards quiet times in the solar wind, since only "clean" cases are counted. Further, the geometric location adjacent to the rarefaction belies the idea that the events are due to convecting disturbances, for then they would be more randomly distributed in location.

The most arresting feature is clearly connected with the selenographic invariance on the lunar surface. The four cases shown in Figure 1 covering a period of 21 months conveys this in particular detail, but the repeated occurrence of events in invariant locations on the moon is demonstrated most clearly by Figures 3 and 4 and Table 1, suggesting that some property of localized regions on the moon is responsible. The sporadic appearance in time shows that a contribution due to changes in the constitutive parameters of the solar wind cannot be completely ruled out. The orientation of the interplanetary magnetic field, the total tensor plasma pressure (see Spreiter et al. [1970] and Schwartz et al. [1969]) and possibly the ion temperature alone [Colburn et al., 1971] may be linked to the appearance. An effect of the interplanetary magnetic field latitude has been detected [Mihalov et al., 1971].

Possible sources of exterior perturbations

If these perturbations arise from an interaction of the solar wind with the moon as the data appear to indicate, then it is plausible to consider whether some form of electromagnetic interaction takes place; a purely gas dynamic interaction is ruled out by the collision-free properties of the solar wind and the small density of any vestigial atmosphere that the moon might possess. Bulk electromagnetic interaction with the moon is divisible into two primary modes associated with transverse magnetic (TM) and transverse electric (TE) excitation [Schubert and Schwartz, 1969; Blank and Sill, 1969]. Both exhibit time dependent behavior and the TM mode is still present in the steady state provided that certain requirements on the bulk electrical conductivity are met [Sonett and Colburn, 1967; 1968]. It is known that the moon is endowed with a substantial global TE excitation while the TM mode is still in doubt [Sonett et al., 1971a,b,c].

The apparent subglobal scale of the source regions as indicated by the maps of Figures 3 and 4 and Table 1 show that the application of the idea of solar wind excitation must now be applied on a smaller scale than hitherto where only the global response was shown. The activation of the TM mode requires that a continuous current path exist through the moon; but it is only necessary that a path be found which crosses the electrical equator (defined by the plane containing $\vec{v}$ and $\vec{B}$ where $\vec{v}$ is the bulk velocity vector of the solar wind and $\vec{B}$ the interplanetary magnetic field vector) so that a potential difference is established [Sonett and Colburn, 1967; Schwartz et al., 1969; Hollweg, 1968]. Additionally it is required that electrical contact be established with the solar wind. Significant asymmetries in the lunar crust showing a variable bulk electrical conductivity would suffice to establish the TM induction locally in the surface, as noted by Hollweg [1970], but an analysis is also presented for local TE mode excitation in "islands" of anomalously high conductivity. Indeed both modes are excited in the presence of a time dependent magnetic field. Nevertheless there are rather special circumstances which must be geochemically established in order for the conductivity conditions to prevail.

Implications for lunar structure

Plutonic activity on the moon is at least as recent as 3.2 billion years ago as determined from Rb/Sr dating [Papanastassiou and Wasserburg, 1970; Compston et al., 1971]; this activity resulted in the flow over significant portions of the lunar surface of sheets of lava forming the marial covering. Although the source regions are likely located deep within the moon, perhaps at depths of several hundreds of kilometers [Ringwood and Essene, 1970], it is not unreasonable to assume that the magmatic material forms geochemically and therefore electrically contiguous regions downwards from the surface to the sources. On the other hand, the highlands are thought to represent older matter from a very early melting [Wood et al., 1970; Urey et al., 1971; Wood, 1971]. The best measurements of the electrical conductivity of lunar material are of the basalts which show anomalously large values [Schwerer et al., 1971]; if the conductivity is dominated by the pyroxenes as suggested by Schwerer et al. [1971], then the surface anorthosites should have a substantially lessened conductivity.

Thus it seems that "islands" of high conductivity on the lunar surface would more readily be associated with the maria where the content of high conductivity basalts should be greater (although see Lamar and McGann [1966]). It would also appear most plausible that if DC current paths were established these ought to include or even be restricted primarily to the maria rather than the highlands. Thus although sufficient evidence is not yet available regarding the appropriate electrical conductivity functions to employ, the most likely conditions would appear to be met if lunar limb interactions favored the maria, provided also that either or both the TM and TE modes were implicated. As the situation now appears to evolve, the inverted conductivity requirements do not favor an inductive mechanism for the origin of the perturbations, provided that the highland matter is shown conclusively to possess substantially lesser conductivity than that of the marial basalts.

Surface observations of permanent magnetism

Permanent magnetism is known to be a common property of lunar material. Numerous rock samples returned to Earth exhibit magnetic fields that could be attributed to thermoremanence (TRM) [Nagata et al., 1970; Runcorn et al., 1970; Strangway et al., 1970; Pearce et al., 1971; Helsley, 1971; Nagata et al., 1971]. These fields are thought to be associated with nearly pure grains of iron of superparamagnetic size [Nagata et al., 1970; Runcorn et al., 1970]. The general belief held is that the magnetism was stabilized at times comparable to the Rb/Sr ages of rocks which differ by 0.5 billion years for Tranquilitatis and Procellarum ranging from 3.2 to 3.7 billion years ago [Papanastassiou et al., 1970; Papanastassiou and Wasserburg, 1970; Compston et al., 1971]. These field sources are likely to be of small scale compared to that of the moon as a whole, but a possible variety of scale sizes are involved. It is known from the Apollo 12 magnetometer that a field of 38 gamma is present at the landing site [Dyal et al., 1970; 1971]. Also the portable magnetometer on Apollo 14 showed two distinct places where fields were present, i.e., at Site A (100 gamma southeast) and Cone Crater (35 gamma southeast) showing therefore that these fields were of small (micro) scale [Dyal et al., 1971]. The supposition is present that the Apollo 12 field is also of small scale.

Scale sizes for lunar magnetism

The present work suggests fields having a larger scale, following Barnes et al. [1971]. The assumption that the magnetic perturbations witnessed by Explorer 35 are due to an interaction of the solar wind with permanently magnetized regions supports the view that the moon tends, everywhere or nearly everywhere, to be magnetized at some level (see also Clay et al. [1971]). There is a bias in the present data towards highland magnetization which suggests that if permanent magnetism is indicated for the source of the solar wind perturbations, then the scale of magnetization of the maria may be considerably smaller than that of the highlands. Alternative suggestions are that an original large scale magnetization of the moon has been much reduced in the marial basins, or possibly that fracturing or shielding is greater there. If it is accepted that the highlands are comprised of anorthositic matter overlying a basement rock of different composition, then the presumed weaker magnetization of the anorthosites requires that the basement rock be the source of the magnetization, implying a sufficient scale size so that the depth is immaterial to the detection. The fields seen at Fra Mauro (Apollo 14) show that the local rocks must be magnetized, for the scale size of the fields is restricted. Either these rocks are from deep within Imbrium, and have preserved their early magnetization in spite of shock modification, or some form of exotic magnetization connected with later cratering is required, but this seems ad hoc and requires a late background field, which is implausible.

Implications for lunar history

A combined magnetization both in the maria and highlands remains somewhat enigmatic at the present time, possibly suggesting repeated episodes of magnetization. However, the detailed magnetic behavior of lunar rocks is still not well understood and such suppositions are tentative at this time. The view that a magnetization episode early in lunar history took place is strongly inferred by the Apollo 14 results, provided that the rocks are subsequently shown to have originated in a basement layer, and are not heavily magnetically modified by the ejection accompanying the formation of Imbrium. If this view is supported by subsequent investigation of the properties of the Apollo 14 rocks, then it seems most plausible to view the Explorer 35 perturbations as arising from magnetization on scales of order 100 km or more of basement rock; the possibility that the anorthosites are magnetized cannot presently be ruled out, however. Telescope observations suggest that the highlands contain significant components that are not anorthositic in nature [Adams and McCord, 1971]. Either would support our inference that the perturbations arise from magnetic anomalies.

It still remains to be explained why the giant maria appear to be deficient in large scale magnetization. One possibility is that these maria, formed by collisional events, have had their highest magnetization later removed as ejecta, but this cannot easily explain the presence of magnetized basalts having ages much less than that of the moon as a whole. One must also explain why the magnetic field appears to be broken up with a variable scale size ranging from perhaps several hundred km downwards, and also why the remanent fields appear to favor equatorial regions so strongly. We can conjecture that the scale size is due to cratering events with a possible addition of internal motions early in lunar history. Such events would introduce a randomization of field directions and intensities, though imperfectly.

It is possible that the statistics, which depend heavily upon the satellite orbits and favor equatorial regions, have introduced an obscure bias in favor of low latitudes. The apparent complete absence of polar perturbations, however, suggests that this feature cannot be exclusively due to statistical bias, but the explanation could lie in the distance dependence discussed previously. Future measurements could show that the magnetization exists everywhere, but that the larger scale events tend to favor the equatorial zone. If the magnetization were due to the existence of an early dipolar lunar dynamo, then large differences should not be found in the latitude dependence of magnetization, as the dipolar source of the fields which presumably were frozen into the material have only a factor of two variation. This statement implies that the entire moon was above the Curie point at the time of onset of the primary magnetization event. On the other hand, if only the outer portion (mantle) were at a sufficiently elevated temperature, then we find the initial magnetization to be confined to a shell. Such magnetization could, in principle, arise either from an internal dynamo or from magnetization while the moon was within the confines of the Earth's magnetosphere, the latter possibly extended at the time beyond the present value (cf. Sonett and Runcorn [1971]). The limitation of the dynamo argument lies in the previous assumption of mantle melting alone, for although a dynamo could be imagined, it would have to operate entirely within the region subject to liquid and solid state convection, presumably an outer shell, which we tentatively identify with a mantle (cf. Runcorn [1967]). Such a dynamo, although plausible, would have to be of a high order and subject to magnetic Reynolds number limitations implying different convection rates than for a dynamo encompassing the whole volume of the moon.

CONCLUSIONS

Earlier results regarding the selenographic invariance of source locations for magnetic field perturbations observed in the solar wind exterior to the lunar cavity signature are further verified and extended. The Mach angle for these perturbations is 7° (13° using cases with plasma data alone); these values are consistent with Mach angles of MHD waves. Data on exterior perturbations show a large decrease in occurrence rate beyond 3.5 lunar radii downstream, and suggest that this decrease is a property of the perturbations rather than a selenographic bias against high latitude locations. An interpretation of the exterior perturbation observations as signatures of magnetized regions on the lunar surface, considering the Apollo 12 and 14 surface magnetic field measurements, is followed. If the source locations are much under 100 km in size, surface fields in the range of a few thousand gamma would be the lower limit permitting direct observation on a single pass with the Ames magnetometer at the Explorer 35 periselene. However, there is no direct evidence for surface fields from constant field data taken in the geomagnetic tail at periselene over inferred source locations. The ages of the field sources should be consistent with, or older than, those based on ages of lunar basalts.

Acknowledgement

We thank Dr. P. M. Cassen for critical comments on the manuscript.

FIGURE CAPTIONS

1. Magnitude of the interplanetary magnetic field in the neighborhood of the diamagnetic cavity on the rear side of the moon. A general level of fluctuations in the field is observed in the data upon which is superimposed the diamagnetic increase in the field (B) and the rarefaction depression on either side of the increase. An anomalous increase (A) in the field is seen to the left of the rarefaction in each of the four cases. In the first and fourth instances an increase (for example, A') is also noted on the right side (satellite exit) but these are excluded from the statistical analysis, in the first case because the amplitude is < 0.7 gamma and in the fourth case because there are many peaks. The selenographic latitude and longitude on the surface of the moon are indicated for projected source locations for each entrance perturbation. The optical shadow region is indicated for each trace. The measured field directions for each case are not presented here in order to simplify the Figure.
2. Idealization of the geometry of the perturbations based upon the hypothesis that they are produced near the limb of the moon and propagate downstream towards the location of Explorer 35. In this illustration the perpendicular to the moon's center is the same as the solar wind terminator.
3. Mercator map of the moon's equatorial regions showing inferred source locations associated with individual perturbations projected upon the surface as indicated on Figure 2. Additional points over those used for the map given in Mihalov et al. [1971] are given, and there are a few deletions. Cases located using plasma data are indicated by triangles. Slash marks indicate source locations due to perturbations observed more than 2.1 lunar radii downstream.

4. Mercator map showing locations of hypothetical sources clustered in 15 × 15 degree regions. There is a tendency to favor the highlands and the equatorial regions of the moon. A correction is made for the number of times the projected source locations could have occurred over particular regions on the lunar surface. The locations of the Apollo 12 and 14 surface magnetic field measurements are indicated with dots; the Apollo 12 location is the western of the two. This Figure extends the previously published one [Mihalov et al., 1971] with additional data.

5. Downstream locations of the perturbations. The circles indicate those cases where the idealized aberration angle of 4° was used when plasma data was absent, while the squares are for those cases where the plasma flow direction was known. All cases are rotated into a common plane though the data is taken at varying latitude. The dashed lines are assumed Mach lines generated by least squares fitting of the data to a straight line separately for the upper (satellite entrance) and lower (exit) cases.

6. Relative amplitude, $\Delta|\vec{B}|/|\vec{B}|$, of the 38 cases of perturbations observed during March 19 to September 29, 1968, plotted against downstream distance in lunar radii using the aberrated solar wind direction. The squares designate perturbations associated with the region at 128° to 144° E longitude and 13° to 25° S latitude.

7. The same cases used in Figure 6 giving the full width at half maximum of the duration of the perturbation plotted against downstream distance. The units of the ordinate are "telemetry sequences" (three sequences comprise 245.4 sec). The squares indicate association with the same restricted region as in Figure 6.

8. The fraction of shadow entrances and exits at various distances downstream from the moon associated with large exterior maxima is given by the circles. The solid line is an aid for the eye. 561 cases from March 18 to October 30, 1968 are used. For the same data, the fraction of shadow entrances and exits with projected source locations within 30° and 45° of the equator is similarly indicated with triangles and squares, respectively, connected by two dashed lines.

9. Particularly quiet Explorer 35 Ames magnetometer geomagnetic tail field data from July 9, 1968 near periselene. The subsatellite location in selenographic coordinates and the altitude is indicated every 5 min. This case contains a 5 min. period centered near periselene over perturbation source locations, with only 3 out of 50 consecutive magnetic field samples indicating a one digitization window change from a background value. The magnetic field is given in solar magnetospheric coordinates. The equatorial plane of this coordinate system is normal to the Z-axis which is the direction normal to the solar direction and in a plane parallel to earth's magnetic dipole containing the solar direction. The field latitude is the angle between the field direction to the equatorial plane, with positive values for northward fields; the field longitude is measured in the equatorial plane, positive counterclockwise from the solar direction when looking from the north.

REFERENCES

Adams, J.B., and T.B. McCord, Alteration of lunar optical properties: Age and composition effects, Science, 171, 567, 1971

Barnes, A., P. Cassen, J.D. Mihalov, and A. Eviatar, Permanent lunar surface magnetism and its deflection of the solar wind, Science, 172, 716, 1971.

Behannon, K.W., Intrinsic magnetic properties of the lunar body, J. Geophys. Res., 73, 7257, 1968.

Blank, J.L., and W.R. Sill, Response of the Moon to the time-varying interplanetary magnetic field, J. Geophys. Res., 74, 736, 1969.

Clay, D.R., M. Neugebauer, and C.W. Snyder, Solar wind observations on the lunar surface with the Apollo 12 ALSEP, Proc. of the Second Lunar Science Conf., The M.I.T. Press (in press), 1971.

Colburn, D.S., R.G. Currie, J.D. Mihalov, and C.P. Sonett, Diamagnetic solar-wind cavity discovered behind Moon, Science, 158, 1040, 1967.

Colburn, D.S., J.D. Mihalov, and C.P. Sonett, Magnetic observations of the lunar cavity, J. Geophys. Res., 76, 2940, 1971.

Compston, W., H. Berry, M.J. Vernon, B.W. Chappell, and M.J. Kaye, Rubidium-strontium chronology and chemistry of lunar material from the Ocean of Storms, Proc. of the Second Lunar Science Conf., The M.I.T. Press (in press), 1971.

Dyal, P., C.W. Parkin, and C.P. Sonett, Apollo 12 magnetometer: Measurement of a steady magnetic field on the surface of the Moon, Science, 169, 762, 1970.

Dyal, P., C.W. Parkin, C.P. Sonett, R.L. DuBois, and G. Simmons, Lunar portable magnetometer experiment, in Apollo 14 Preliminary Science Report, NASA, Washington, (in press) 1971.

Helsley, C.E., Evidence for an ancient lunar magnetic field, Proc. of the Second Lunar Science Conf., The M.I.T. Press (in press), 1971.

Hollweg, J.V., Interaction of the solar wind with the Moon and formation of a lunar limb shock wave, J. Geophys. Res., 73, 7269, 1968.

Hollweg, J.V., Lunar conducting islands and formation of a lunar limb shock wave, J. Geophys. Res., 75, 1209, 1970.

Jeffrey, A., and T. Taniuti, Non-Linear Wave Propagation, Academic Press, New York, 1964.

Lamar, D.L., and J. McGann, Shape and internal structure of the Moon, Icarus, 5, 10, 1966.

Mihalov, J.D., C.P. Sonett, J.H. Binsack, and M.D. Moutsoulas, Possible fossil lunar magnetism inferred from satellite data, Science, 171, 892, 1971.

Mihalov, J.D., and C.P. Sonett, Neue Untersuchungen des lunaren Eigenmagnetismus, submitted to Umschau in Wissenschaft und Technik, 1971.

Nagata, T., Y. Ishikawa, H. Kinoshita, M. Kono, Y. Syono, and R.M. Fisher, Magnetic properties and natural remanent magnetization of lunar materials, Geochim. et Cosmochim. Acta, Suppl. I, 2325, 1970.

Nagata, T., R.M. Fisher, F.C. Schwerer, M.D. Fuller, and J.R. Dunn, Magnetic properties and remanent magnetization of Apollo 12 lunar materials and Apollo 11 lunar microbreccia, Proc. of the Second Lunar Science Conf., The M.I.T. Press (in press), 1971.

Ness, N.F., K.W. Behannon, C.S. Scearce, and S.C. Cantarano, Early results from the magnetic field experiment on lunar Explorer 35, J. Geophysical Res., 72, 5769, 1967.

Ness, N.F., K.W. Behannon, H.E. Taylor, and Y.C. Whang, Perturbations of the interplanetary magnetic field by the lunar wake, J. Geophys. Res., 73, 3421, 1968.

Ness, N.F., and K.W. Schatten, Detection of interplanetary magnetic field fluctuations stimulated by the lunar wake, J. Geophys. Res., 74, 6425, 1969.

Papanastassiou, D.A., G.J. Wasserburg, and D.S. Burnett, Rb-Sr ages of lunar rocks from the Sea of Tranquility, Earth and Planet. Sci. Ltrs., 8, 1, 1970.

Papanastassiou, D.A., and G.J. Wasserburg, Rb-Sr ages from the Ocean of Storms, Earth and Planet. Sci. Ltrs., 8, 269, 1970.

Papanastassiou, D.A., and G.J. Wasserburg, Lunar chronology and evolution from Rb-Sr studies of Apollo 11 and 12 samples, Earth and Planet. Sci. Ltrs., 11, 37, 1971.

Pearce, G.W., D.W. Strangway, and E.E. Larson, Magnetism of two Apollo 12 igneous rocks, Proc. of the Second Lunar Science Conf., The M.I.T. Press (in press), 1971.

Ringwood, A.E., and E. Essene, Petrogenesis of Apollo 11 basalts, internal constitution and origin of the Moon, Geochim. et Cosmochim. Acta, Suppl. I, 769, 1970.

Runcorn, S.K., Convection in the Moon and the existence of a lunar core, Proc. Roy. Soc., A296, 270, 1967.

Runcorn, S.K., D.W. Collinson, W. O'Reilly, M.H. Battey, A. Stephenson, J.M. Jones, A.J. Manson, and P.W. Readman, Magnetic properties of Apollo 11 lunar samples, Geochim. et Cosmochim. Acta, Suppl. I, 2369, 1970.

Schubert, G., and K. Schwartz, A theory for the interpretation of lunar surface magnetometer data, The Moon, 1, 106, 1969.

Schwartz, K., C.P. Sonett, and D.S. Colburn, Unipolar induction in the Moon and a lunar limb shock mechanism, The Moon, 1, 7, 1969.

Schwerer, F.C., T. Nagata, and R.M. Fisher, Electrical conductivity of lunar surface rocks and chondritic meteorites, The Moon (in press), 1971.

Siscoe, G.L., E.F. Lyon, J.H. Binsack, and H.S. Bridge, Experimental evidence for a detached lunar compression wave, J. Geophys. Res., 74, 59, 1969.

Sonett, C.P., Modulation and sampling of hydromagnetic radiation, in Space Research VI, edited by R.L. Smith-Rose, Spartan Books, Washington, 1966.

Sonett, C.P., and D.S. Colburn, Establishment of a lunar unipolar generator and associated shock and wake by the solar wind, Nature, 216, 340, 1967.

Sonett, C.P., D.S. Colburn, and R.G. Currie, The intrinsic magnetic field of the Moon, J. Geophys. Res., 72, 5503, 1967.

Sonett, C.P., Multirate sampling and generalized alias as a source of errors in magnetometer experiments, IEEE Trans. Geosci. Electron., GE-6, 126, 1968.

Sonett, C.P., and D.S. Colburn, The principle of solar wind induced planetary dynamos, Phys. Earth and Planet. Interiors, 1, 326, 1968.

Sonett, C.P., and S.K. Runcorn, How to use magnetic fields for fun and profit, Comm. on Astrophys. and Space Phys. (in press), 1971.

Sonett, C.P., D.S. Colburn, P. Dyal, C.W. Parkin, B.F. Smith, G. Schubert, and K. Schwartz, Lunar electrical conductivity profile, Nature, 230, 359, 1971a.

Sonett, C.P., P. Dyal, C.W. Parkin, D.S. Colburn, J.D. Mihalov, and B.F. Smith, Whole body response of the Moon to electromagnetic induction by the solar wind, Science, 172, 256, 1971c.

Sonett, C.P., G. Schubert, B.F. Smith, K. Schwartz, and D.S. Colburn, Lunar electrical conductivity from Apollo 12 magnetometer measurements: Compositional and thermal inferences, Proc. of the Second Lunar Science Conf., The M.I.T. Press (in press), 1971b.

Spreiter, J.R., M.C. Marsh, and A.L. Summers, Hydromagnetic aspects of solar wind flow past the Moon, Cosmic Electrodynamics, 1, 5, 1970.

Strangway, D.W., E.E. Larson, and G.W. Pearce, Magnetic studies of lunar samples - breccia and fines, Geochim. et Cosmochim. Acta, Suppl. I, 2435, 1970.

Urey, H.C., K. Marti, J.W. Hawkins, and M.K. Liu, Model history of the lunar surface, Proc. of the Second Lunar Science Conf., The M.I.T. Press (in press), 1971.

Whang, Y.C., Theoretical study of the magnetic field in the lunar wake, Phys. Fluids, 11, 1713, 1968.

Whang, Y.C., Field and plasma in the lunar wake, Phys. Rev., 186, 143, 1969.

Whang, Y.C., and N.F. Ness, Observations and interpretation of the lunar Mach cone, J. Geophys. Res., 75, 6002, 1970.

Wood, J.A., Thermal history and early magmatism in the Moon, in The Geophysical Interpretation of the Moon, ed. G. Simmons, in press, 1971.

Wood, J.A., J.S. Dickey, Jr., U.B. Marvin, and B.N. Powell, Lunar anorthosites and a geophysical model of the Moon, Geochim. et Cosmochim. Acta, Suppl. I, 965, 1970.

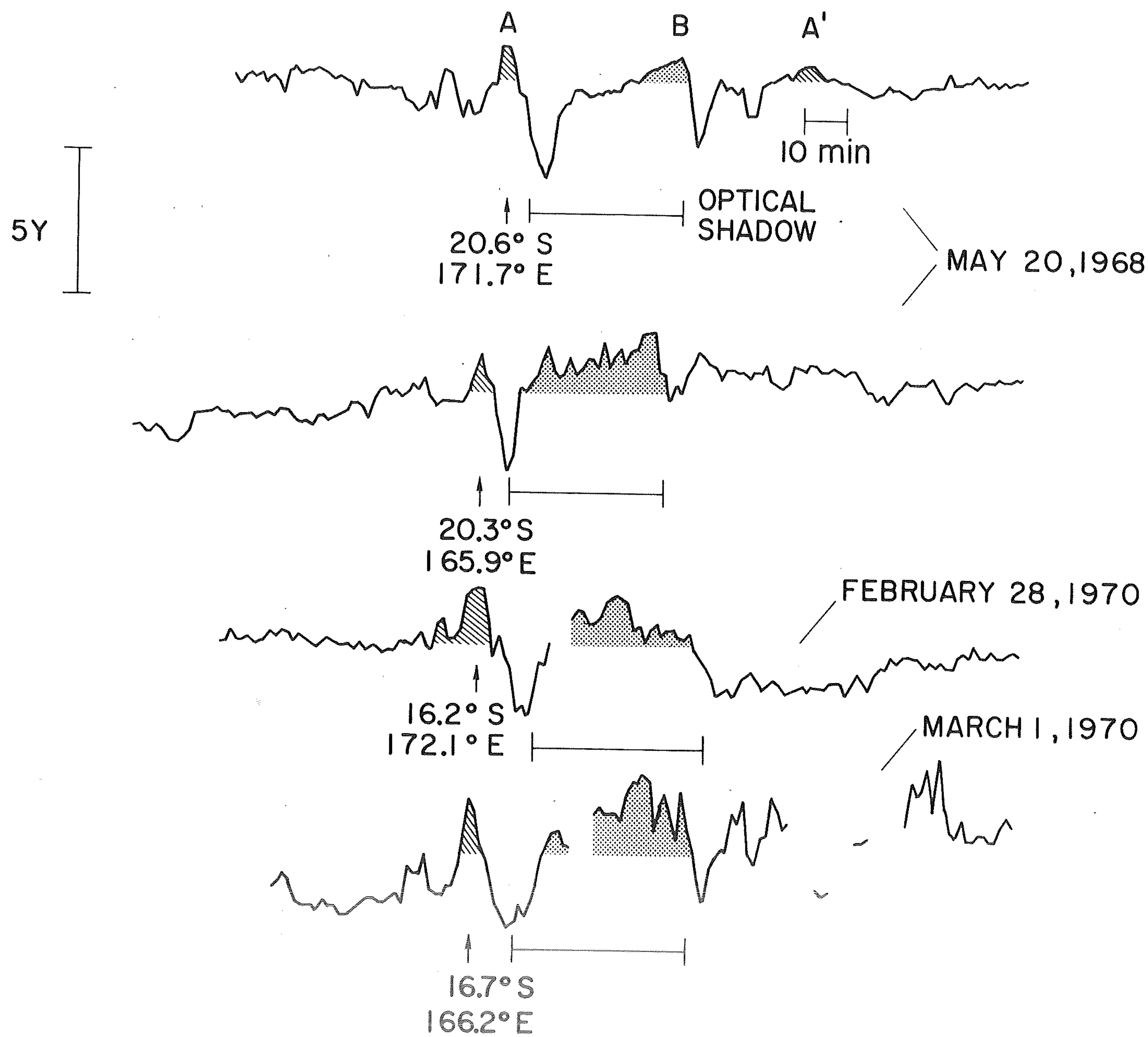

Figure 1

NATIONAL AERONAUTICS AND SPACE ADMINISTRATION
AMES RESEARCH CENTER, MOFFETT FIELD, CALIFORNIA

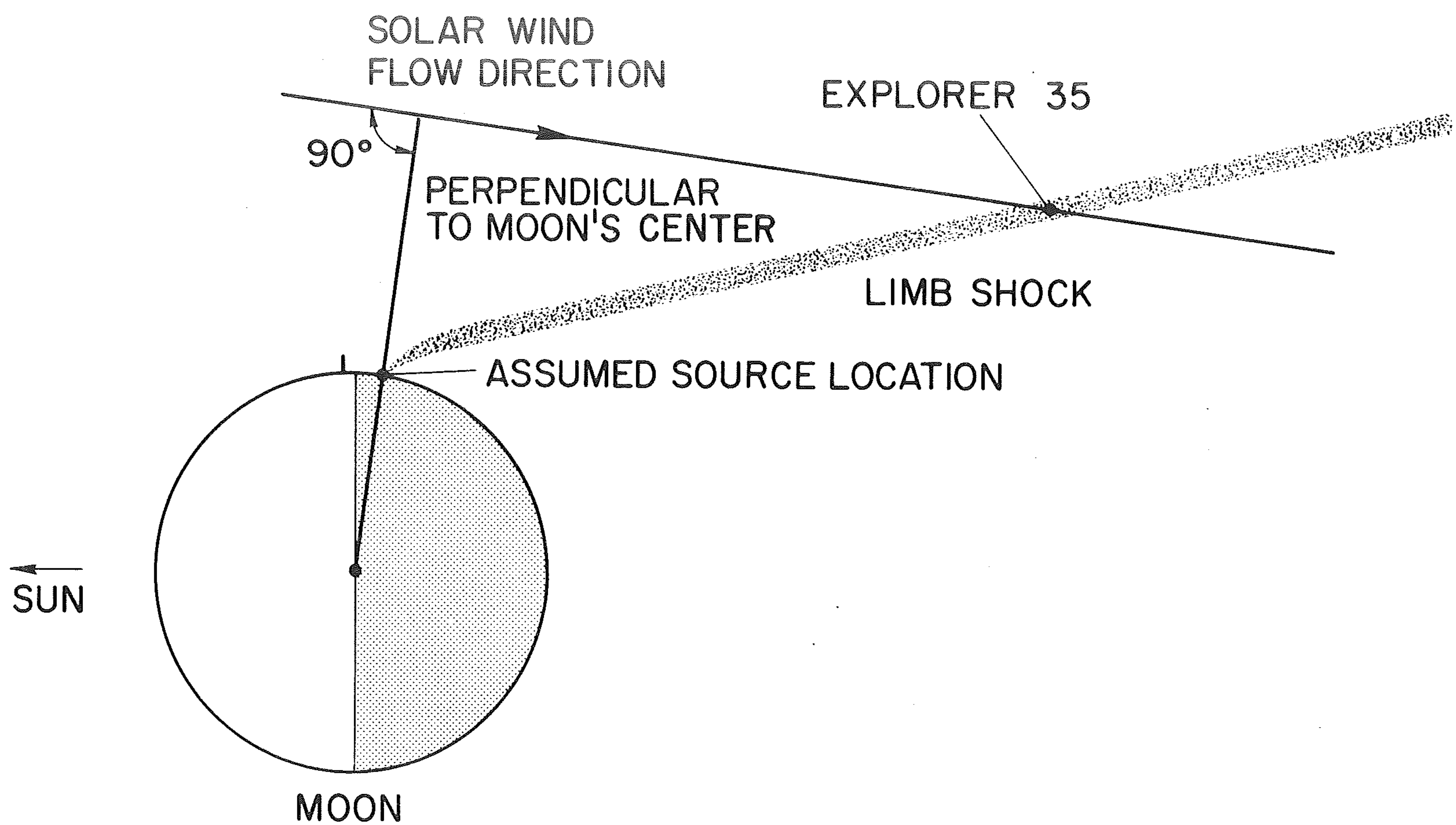

Figure 2

NATIONAL AERONAUTICS AND SPACE ADMINISTRATION
AMES RESEARCH CENTER, MOFFETT FIELD, CALIFORNIA

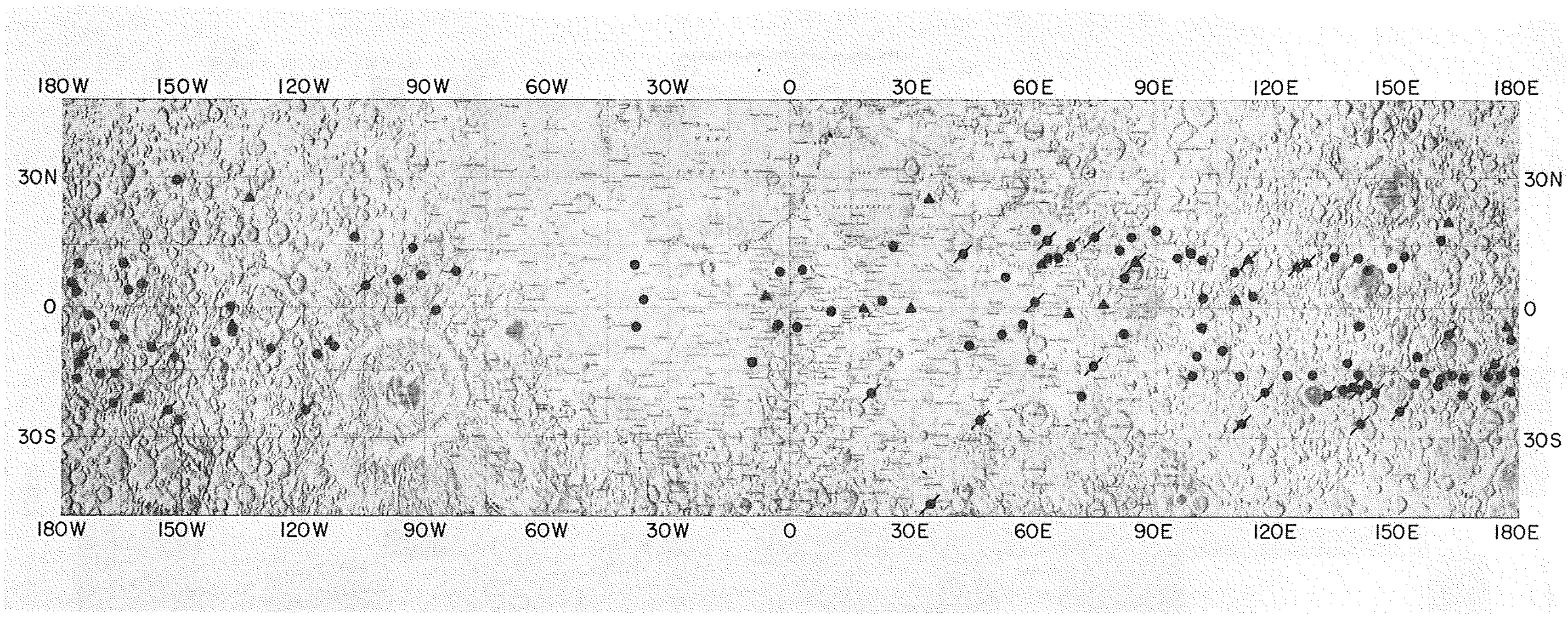
180W
150W
120W
90W
60W
30W
0
30E
60E
90E
120E
150E
180E
30N
0
30S

Figure 3.

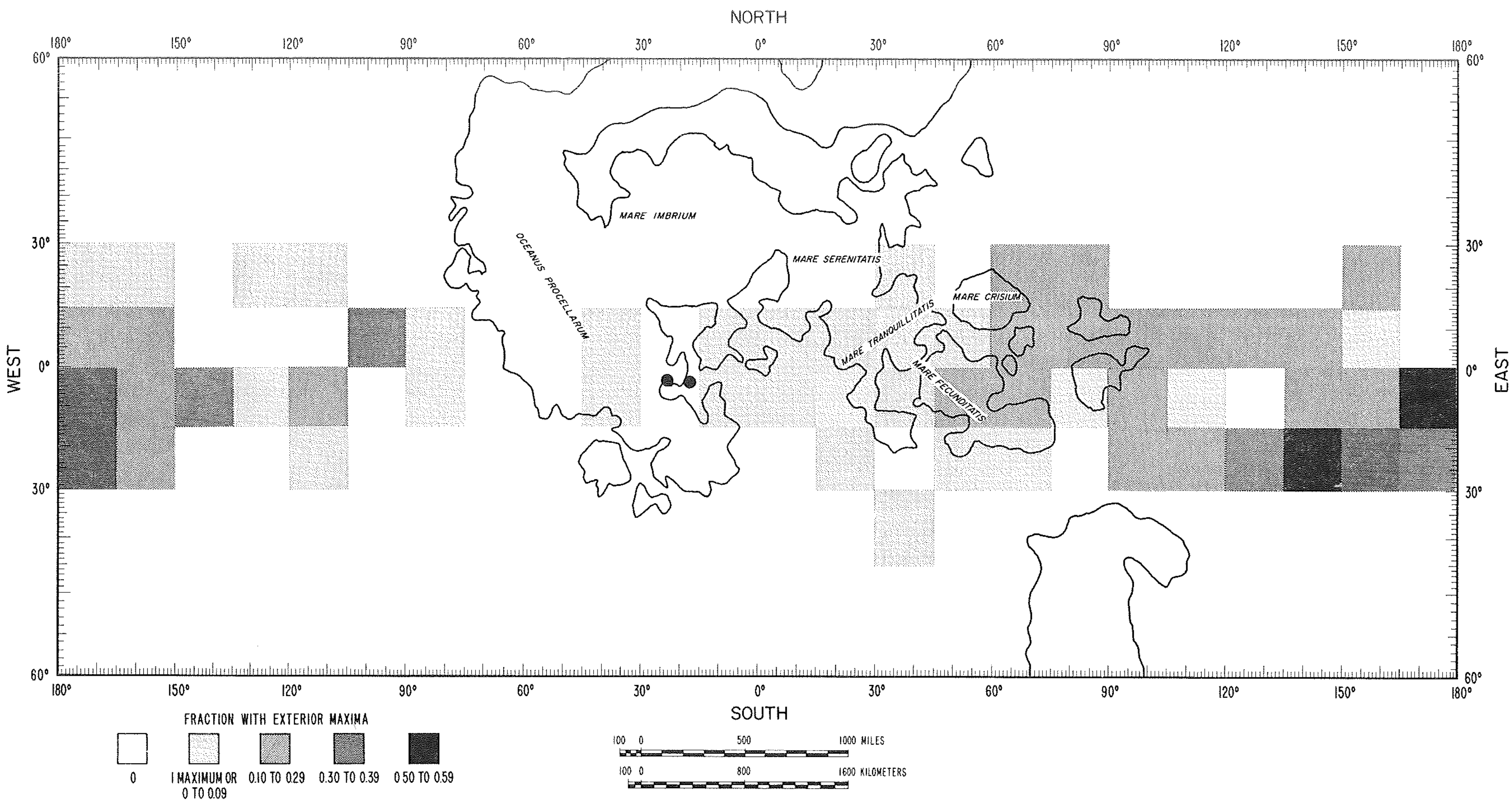
NORTH
SOUTH
WEST
EAST
MARE IMBRIUM
OCEANUS PROCELLARUM
MARE SERENITATIS
MARE CRISIUM
MARE TRANQUILLITATIS
MARE FECUNDITATIS
FRACTION WITH EXTERIOR MAXIMA
0
1 MAXIMUM OR 0 TO 0.09
0.10 TO 0.29
0.30 TO 0.39
0.50 TO 0.59
100 0 500 1000 MILES
100 0 800 1600 KILOMETERS

Figure 4.

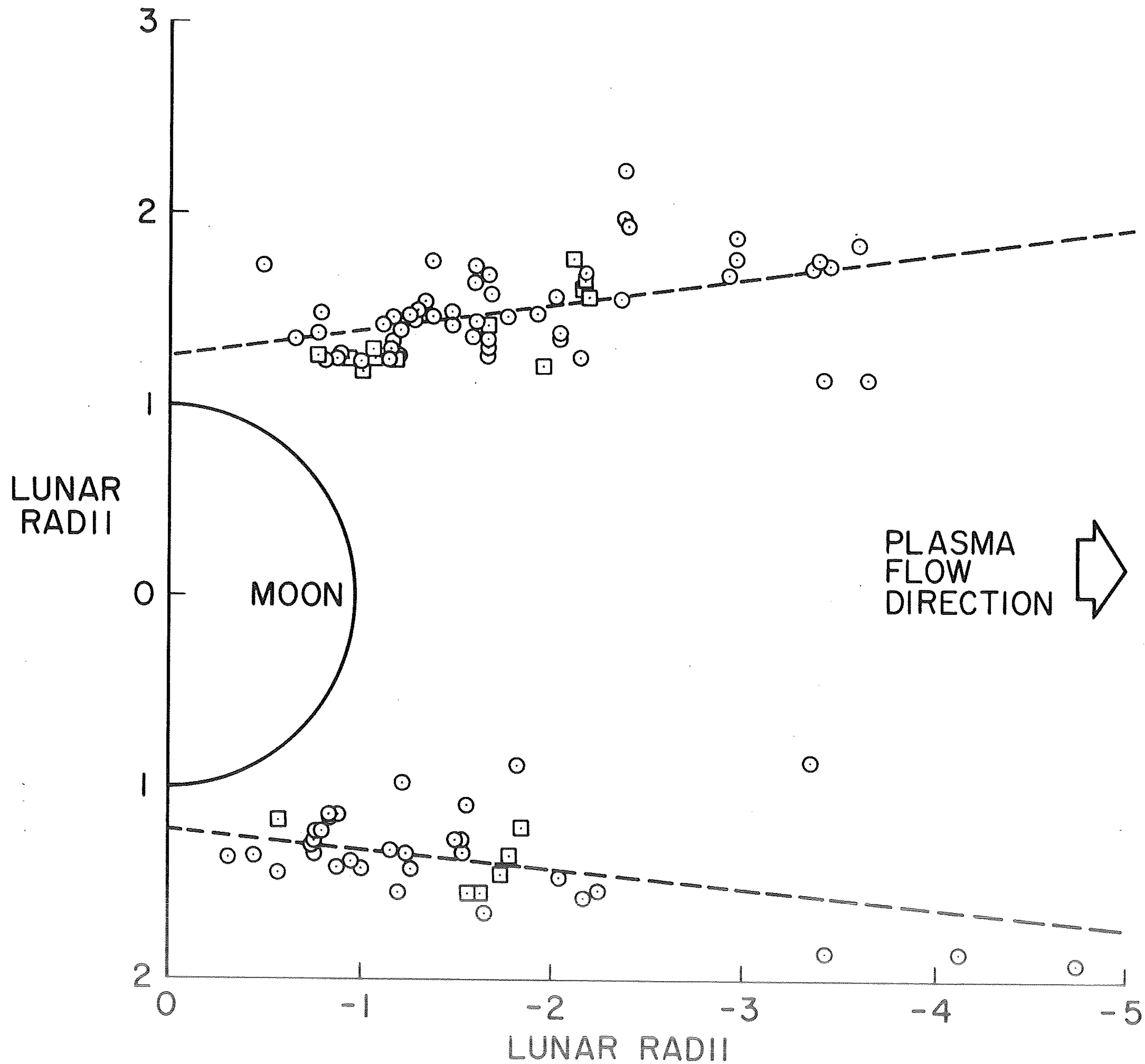
3
2
1
0
1
2
LUNAR
RADII
MOON
PLASMA
FLOW
DIRECTION
0
-1
-2
-3
-4
-5
LUNAR RADII

Figure 5

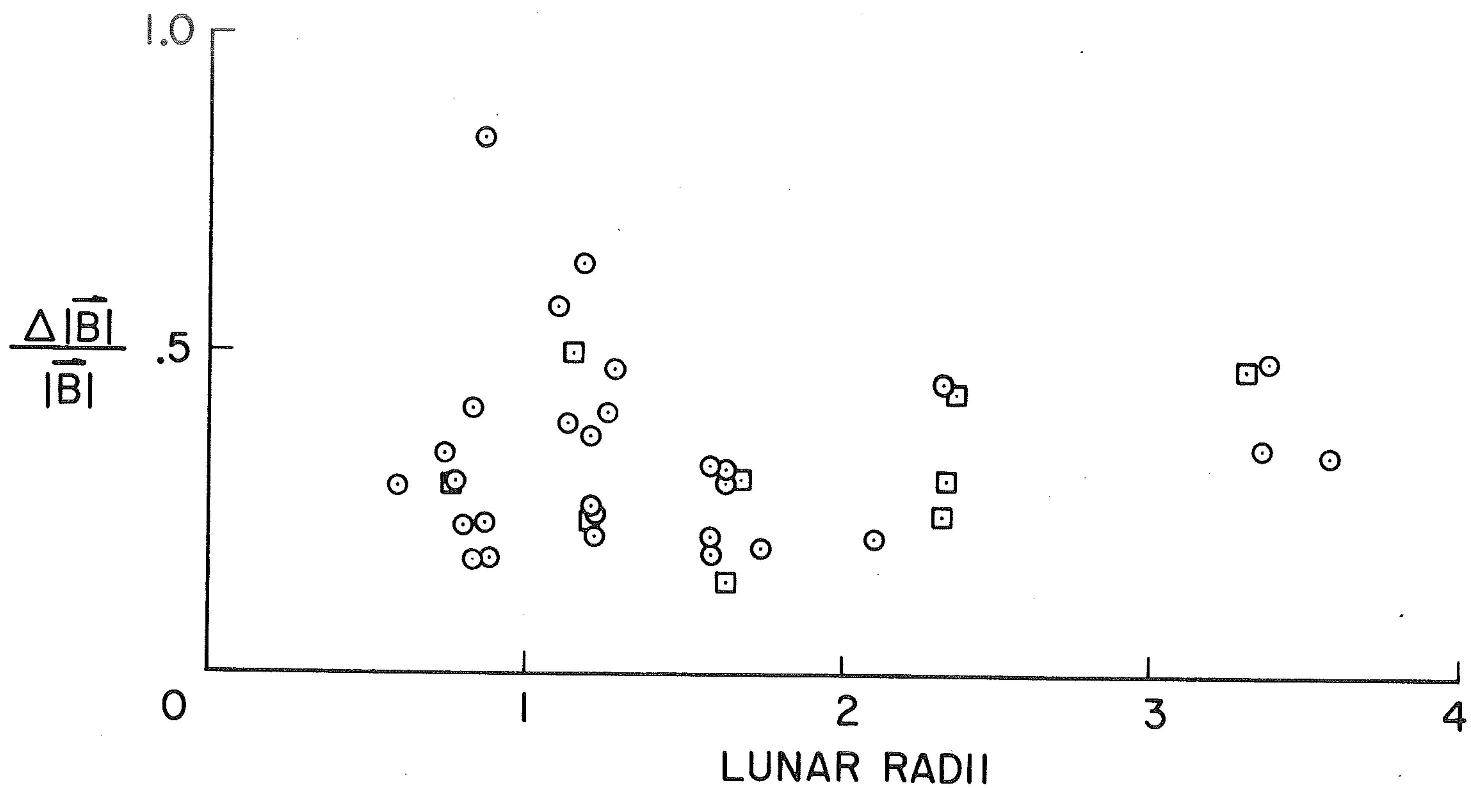

Figure 6

NATIONAL AERONAUTICS AND SPACE ADMINISTRATION
AMES RESEARCH CENTER, MOFFETT FIELD, CALIFORNIA

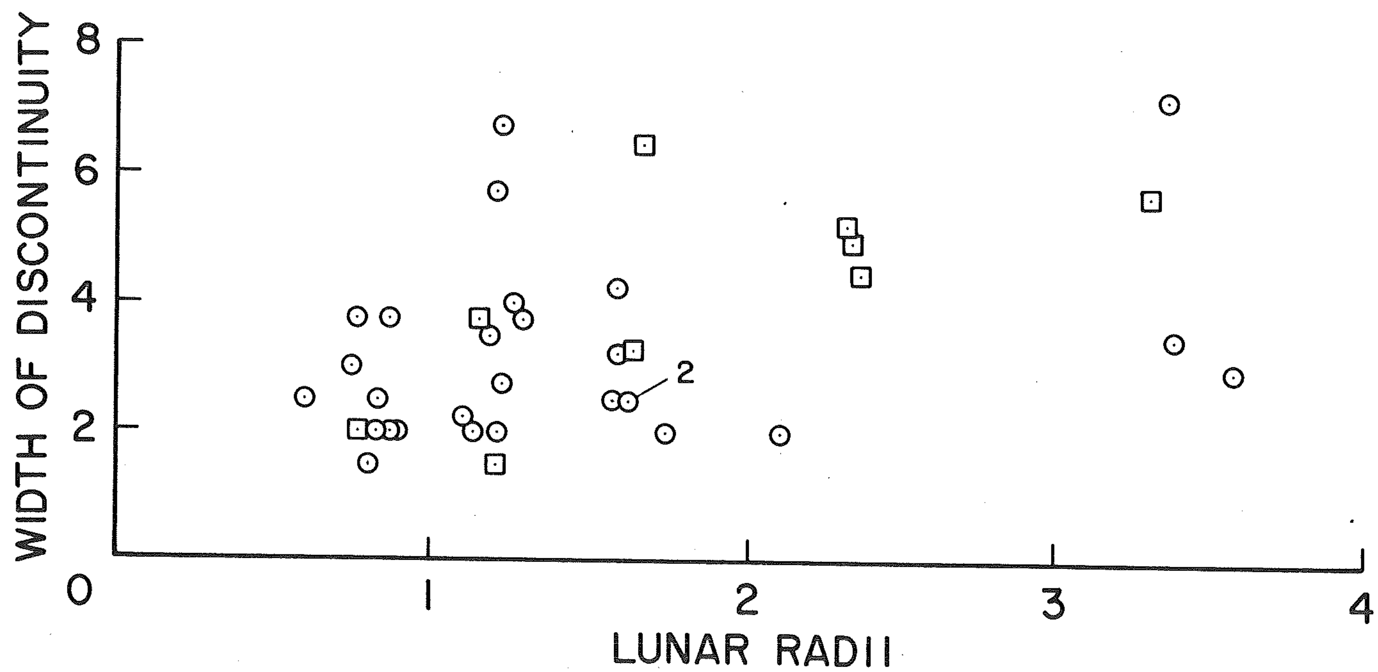

Figure 7

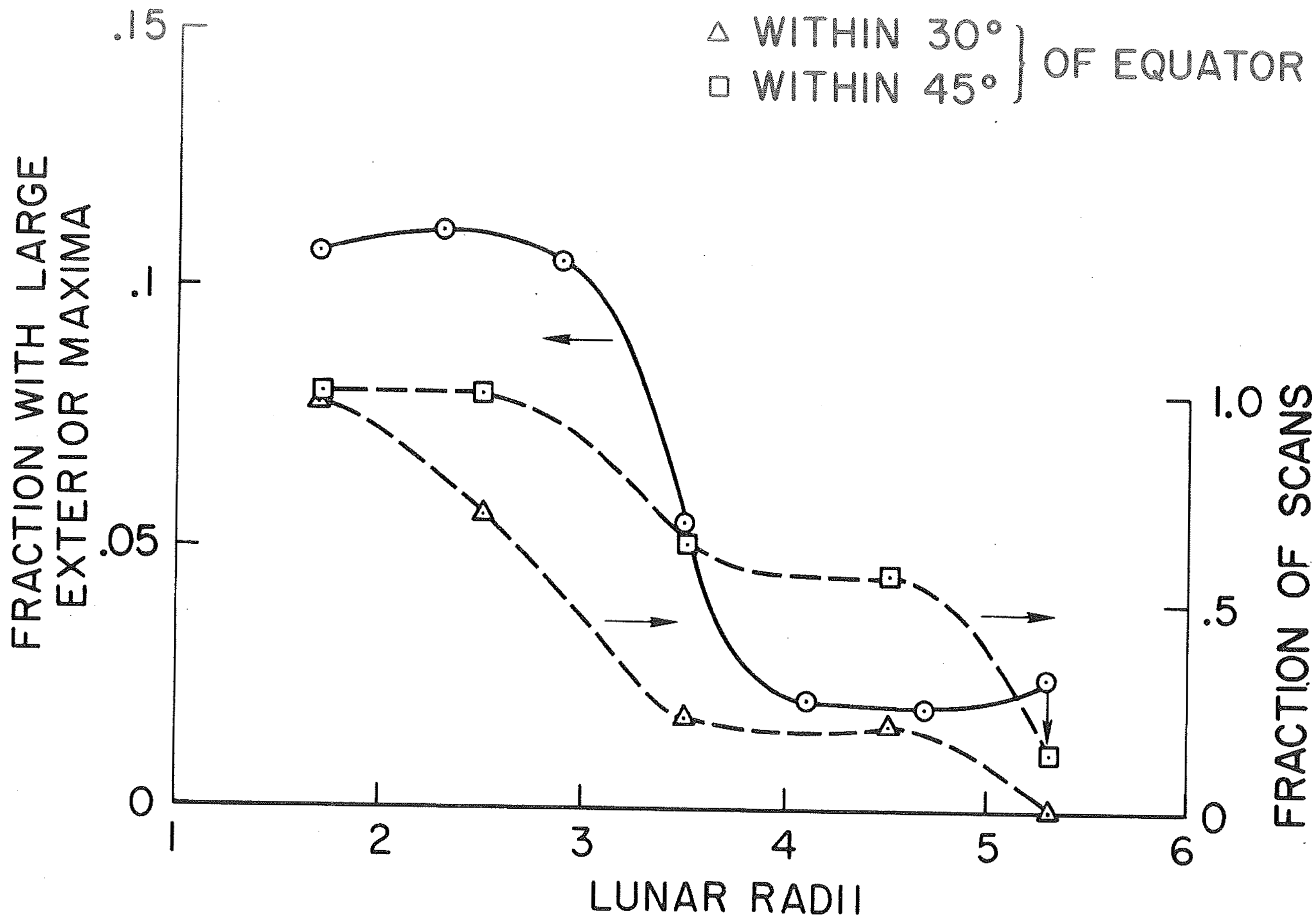

Figure 8

NATIONAL AERONAUTICS AND SPACE ADMINISTRATION
AMES RESEARCH CENTER, MOFFETT FIELD, CALIFORNIA

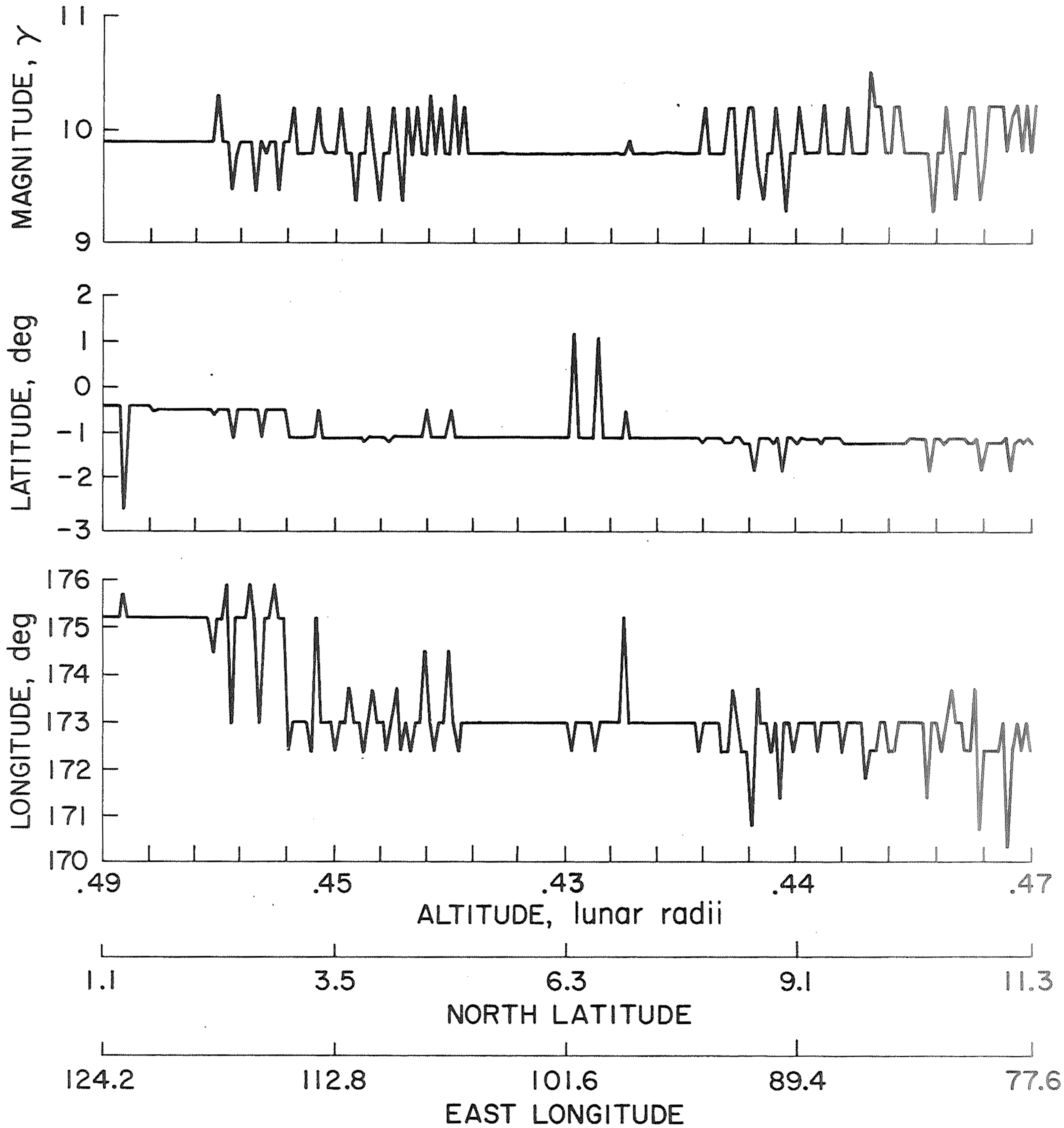
MAGNITUDE, γ
11
10
9
LATITUDE, deg
2
1
0
-1
-2
-3
LONGITUDE, deg
176
175
174
173
172
171
170
.49
.45
.43
.44
.47
ALTITUDE, lunar radii
1.1
3.5
6.3
9.1
11.3
NORTH LATITUDE
124.2
112.8
101.6
89.4
77.6
EAST LONGITUDE

Figure 9